US010642010B2

(12) **United States Patent**
Zhu et al.

(10) **Patent No.: US 10,642,010 B2**
(45) **Date of Patent: May 5, 2020**

(54) **OFF-AXIS HYBRID SURFACE THREE-MIRROR OPTICAL SYSTEM**

(71) Applicants: **Tsinghua University**, Beijing (CN); **HON HAI PRECISION INDUSTRY CO., LTD.**, New Taipei (TW)

(72) Inventors: **Jun Zhu**, Beijing (CN); **Tong-Tong Gong**, Beijing (CN); **Guo-Fan Jin**, Beijing (CN); **Shou-Shan Fan**, Beijing (CN)

(73) Assignees: **Tsinghua University**, Beijing (CN); **HON HAI PRECISION INDUSTRY CO., LTD.**, New Taipei (TW)

(*) Notice: Subject to any disclaimer, the term of this patent is extended or adjusted under 35 U.S.C. 154(b) by 195 days.

(21) Appl. No.: **15/842,834**

(22) Filed: **Dec. 14, 2017**

(65) **Prior Publication Data**

US 2018/0210180 A1 Jul. 26, 2018

(30) **Foreign Application Priority Data**

Jan. 24, 2017 (CN) 2017 1 0059417

(51) **Int. Cl.**
G02B 17/06 (2006.01)
G02B 27/00 (2006.01)

(52) **U.S. Cl.**
CPC ***G02B 17/0642*** (2013.01); ***G02B 17/0621*** (2013.01); ***G02B 27/0012*** (2013.01)

(58) **Field of Classification Search**
CPC G02B 17/0642; G02B 17/0621; G02B 27/0012
USPC 359/858
See application file for complete search history.

(56) **References Cited**

U.S. PATENT DOCUMENTS

2015/0253552 A1* 9/2015 Zhu G01J 1/0414 250/216

FOREIGN PATENT DOCUMENTS

CN 103246053 A 8/2013

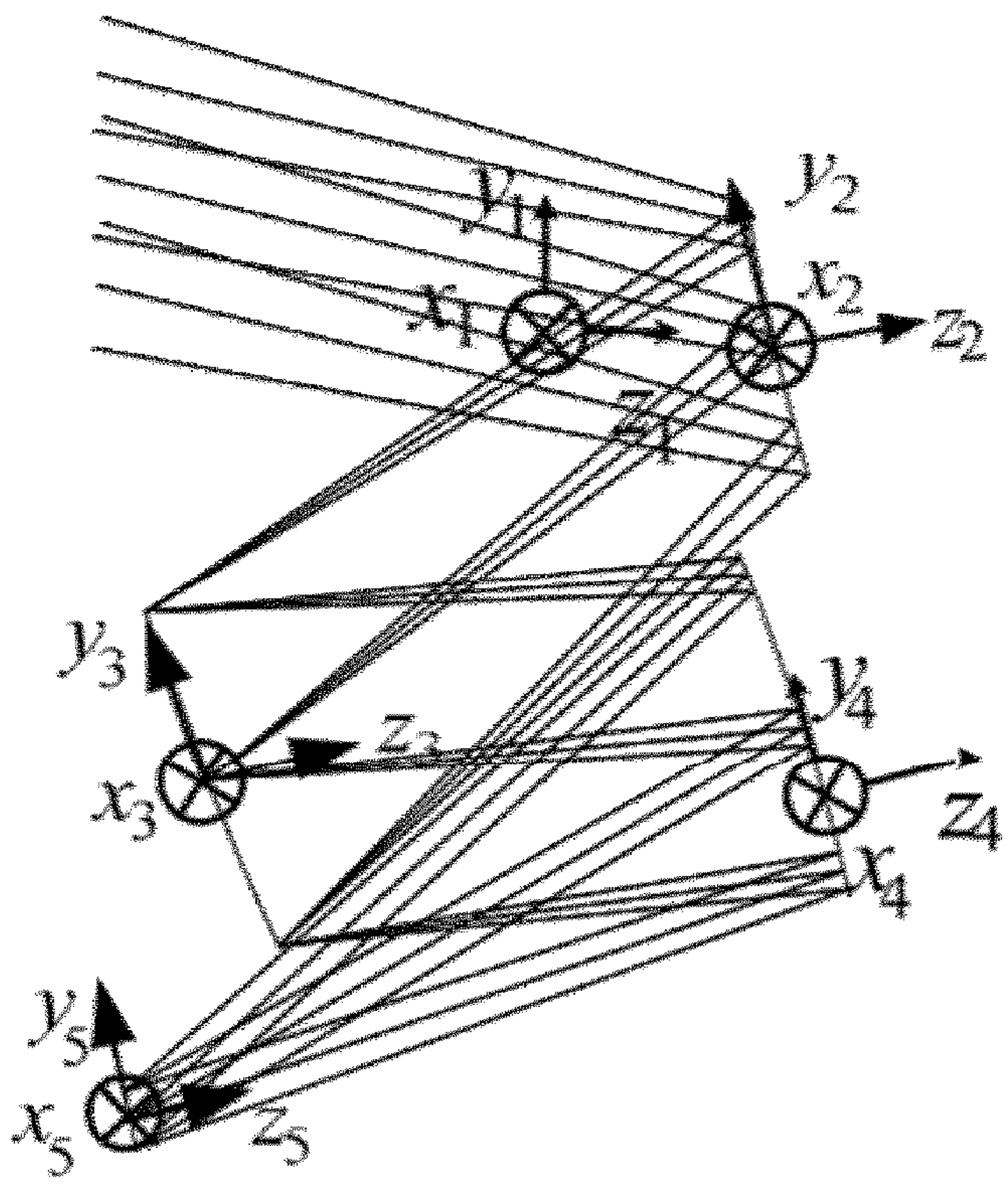
* cited by examiner

Primary Examiner — Stephone B Allen
Assistant Examiner — Rahman Abdur
(74) *Attorney, Agent, or Firm* — ScienBiziP, P.C.

(57) **ABSTRACT**

An off-axis hybrid surface three-mirror optical system comprises a primary mirror, a secondary mirror, a tertiary mirror, and an image sensor. A reflective surface of the primary mirror is a sixth-order polynomial freeform surface of xy. A reflective surface of the secondary mirror is a sixth-order polynomial aspheric surface of xy. A reflective surface of the a tertiary mirror is a spherical surface of xy.

19 Claims, 12 Drawing Sheets



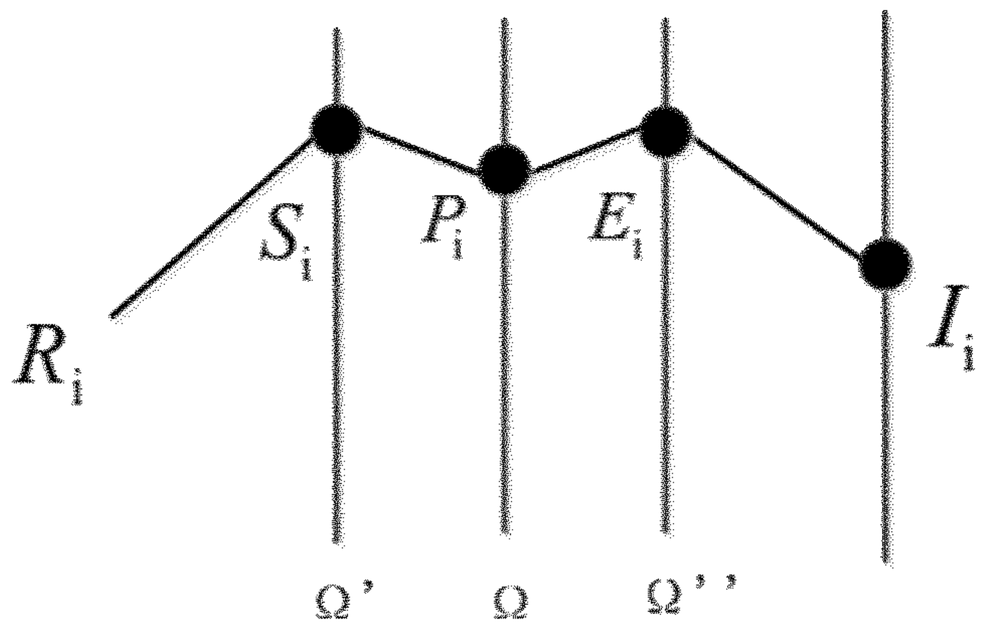


FIG. 1

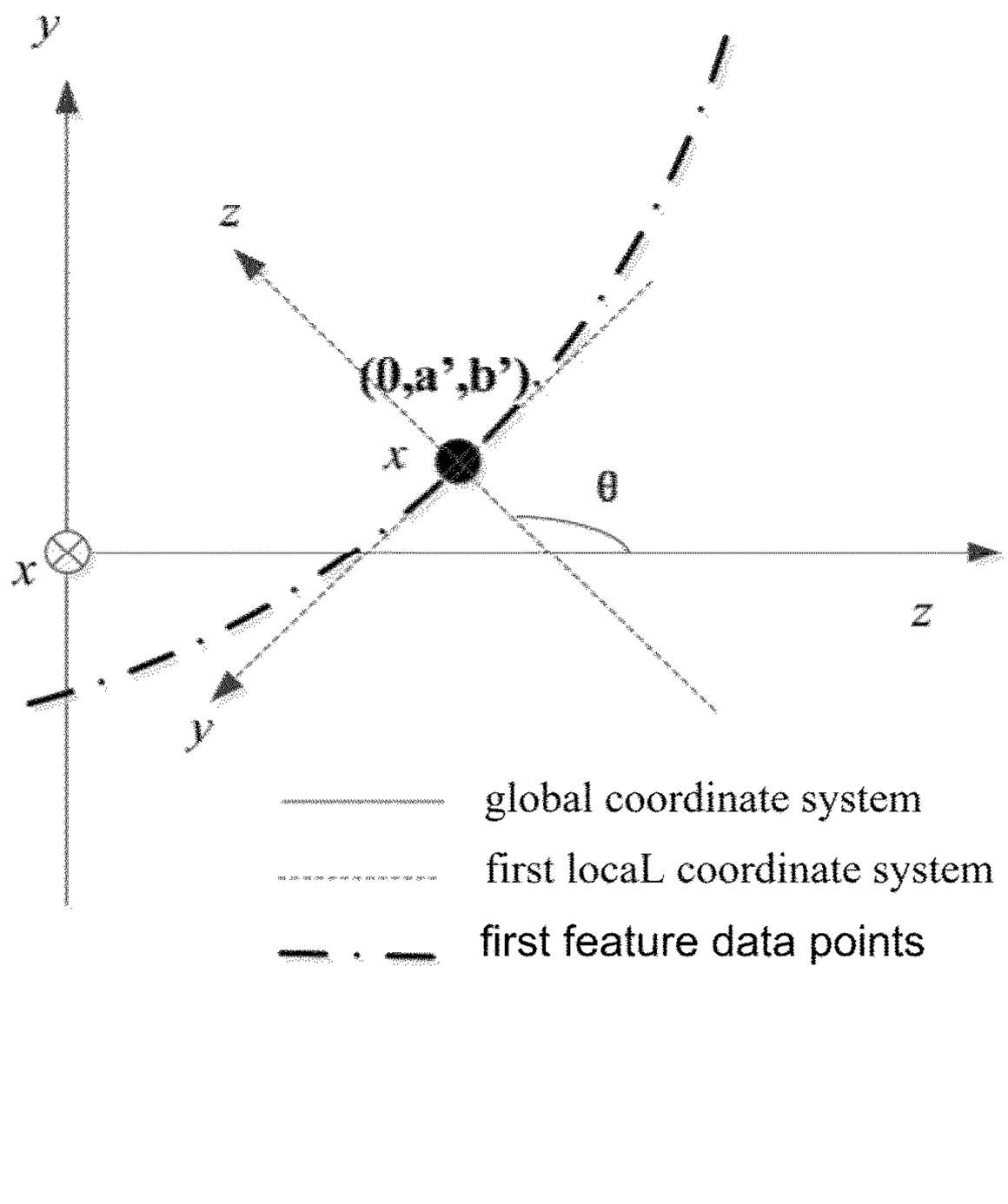

y
z
(0,a',b'),
x
θ
x
z
y
global coordinate system
first locaL coordinate system
first feature data points

FIG.2

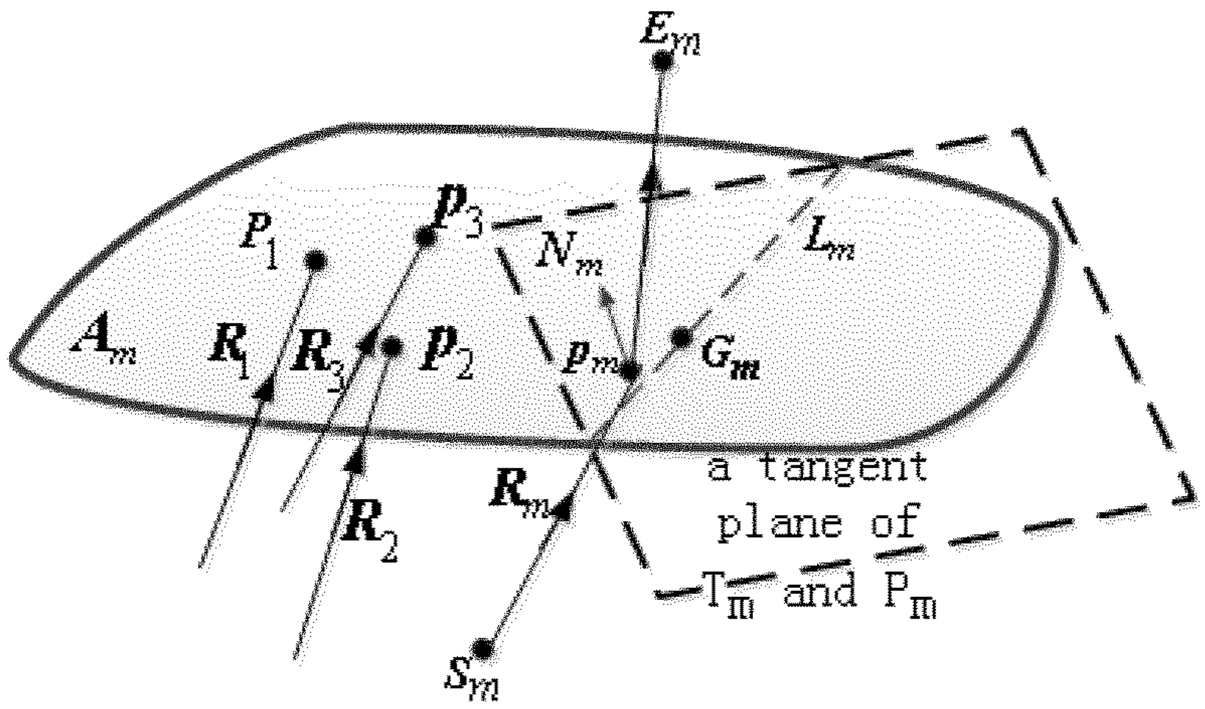

E_m
P_1
P_3
N_m
L_m
A_m
R_1
R_3
P_2
p_m
G_m
R_m
R_2
a tangent plane of T_m and P_m
S_m

FIG.3

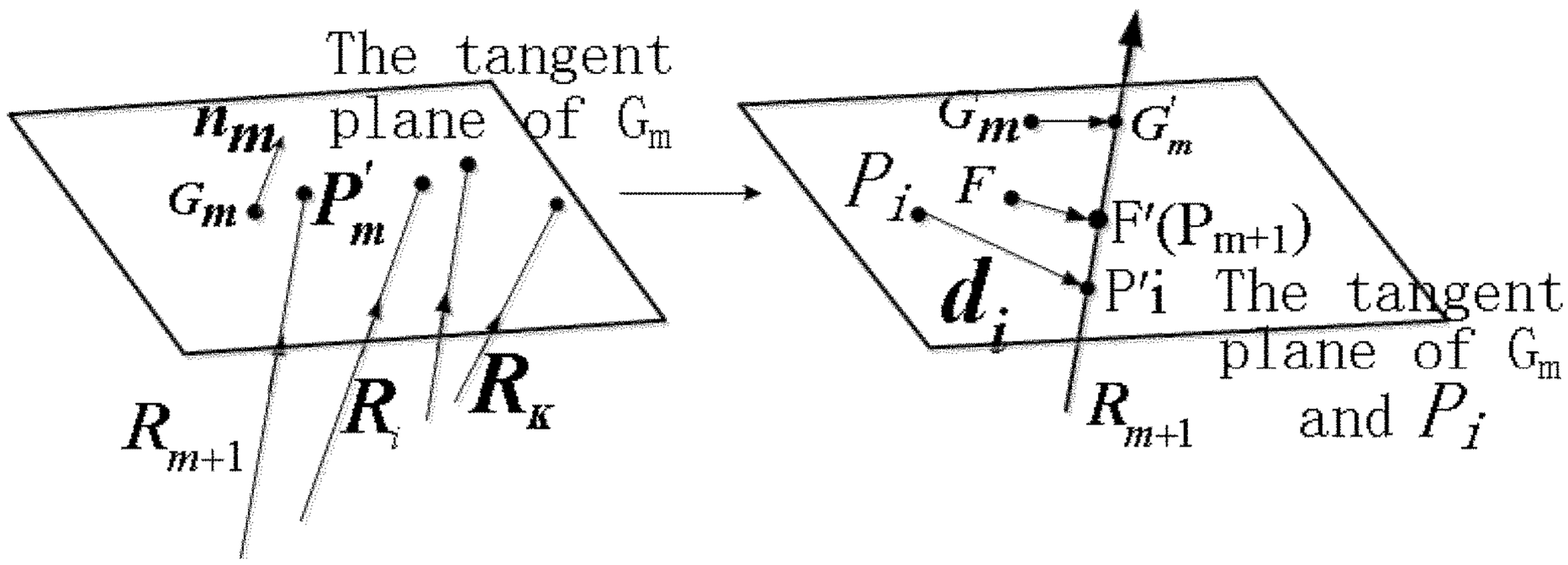

The tangent plane of G_m
n_m
G_m
P'_m
R_{m+1}
R_i
R_K
G_m
G'_m
P_i
F
$F'(P_{m+1})$
d_i
$P'i$
The tangent plane of G_m and P_i
R_{m+1}

FIG.4

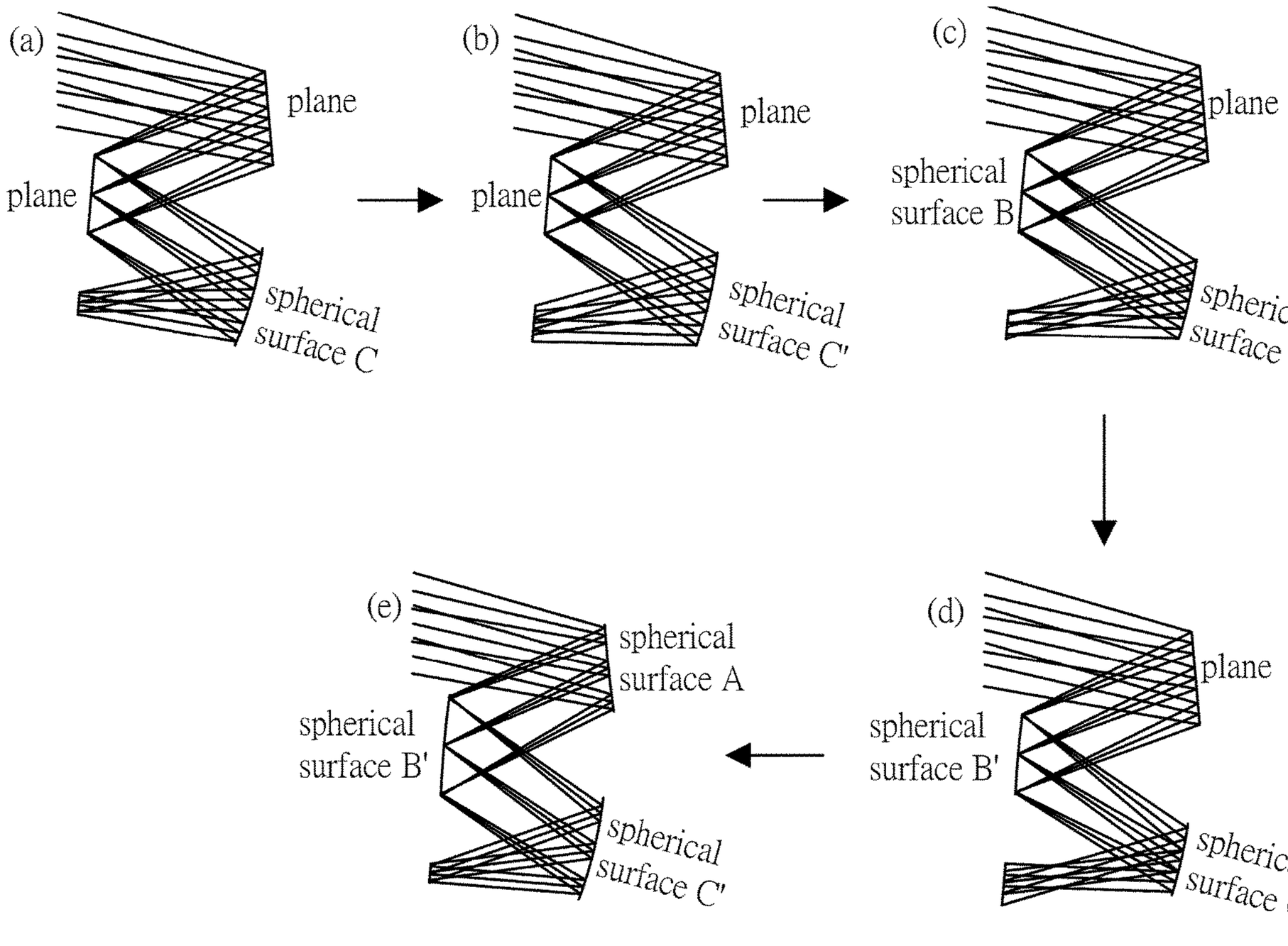

(a)
plane
plane
spherical surface C
(b)
plane
plane
spherical surface C'
(c)
plane
spherical surface B
spherical surface C'
(d)
plane
spherical surface B'
spherical surface C'
(e)
spherical surface A
spherical surface B'
spherical surface C'

FIG.5

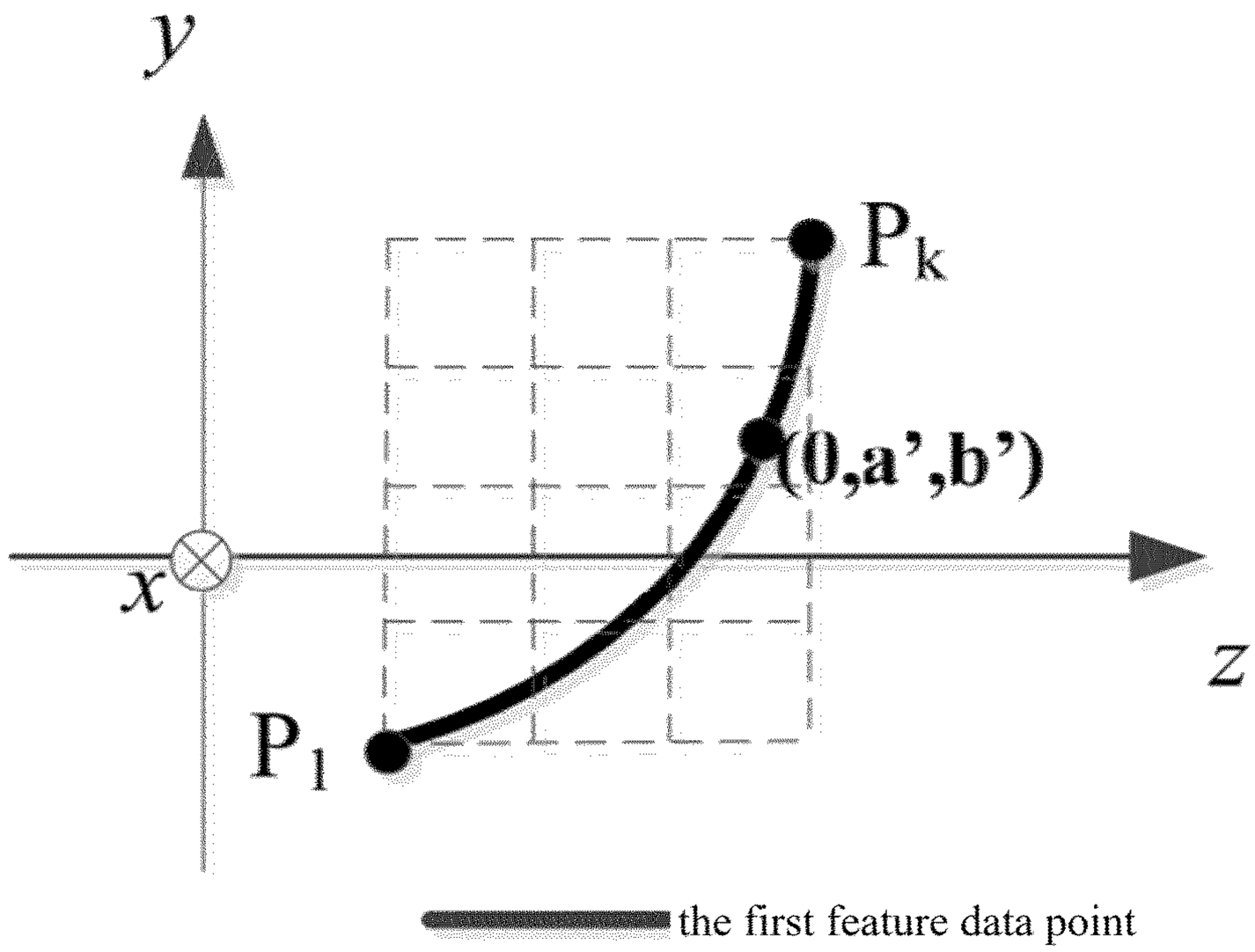


FIG.6

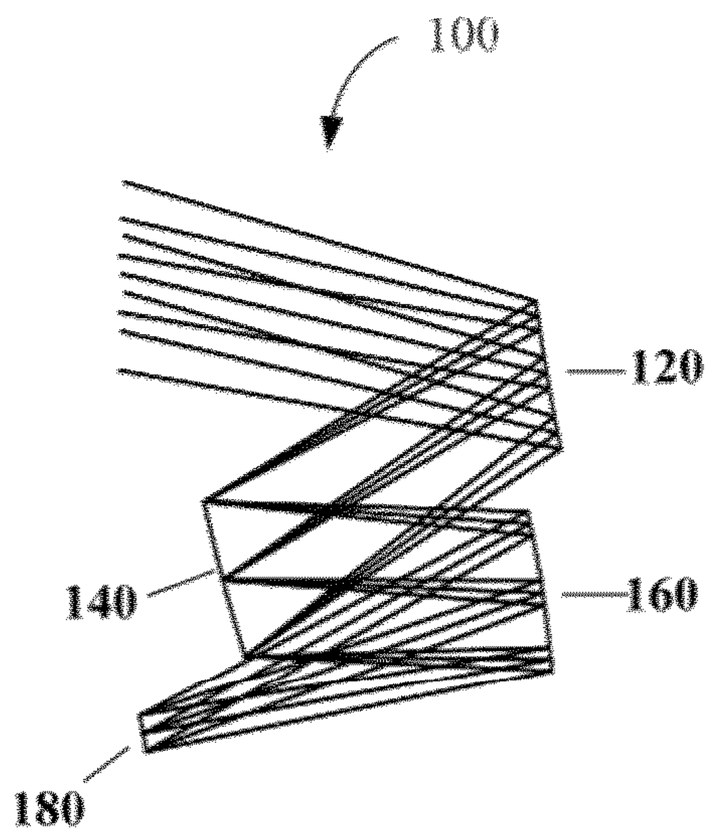


FIG.7

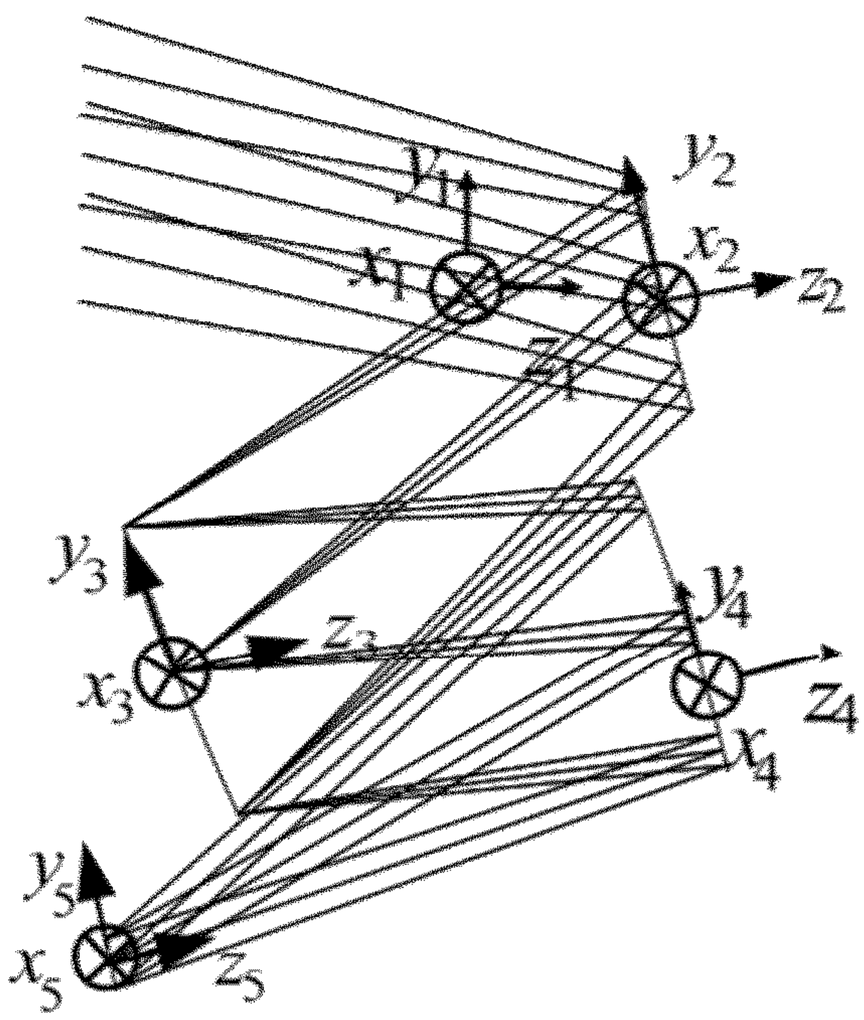


FIG.8

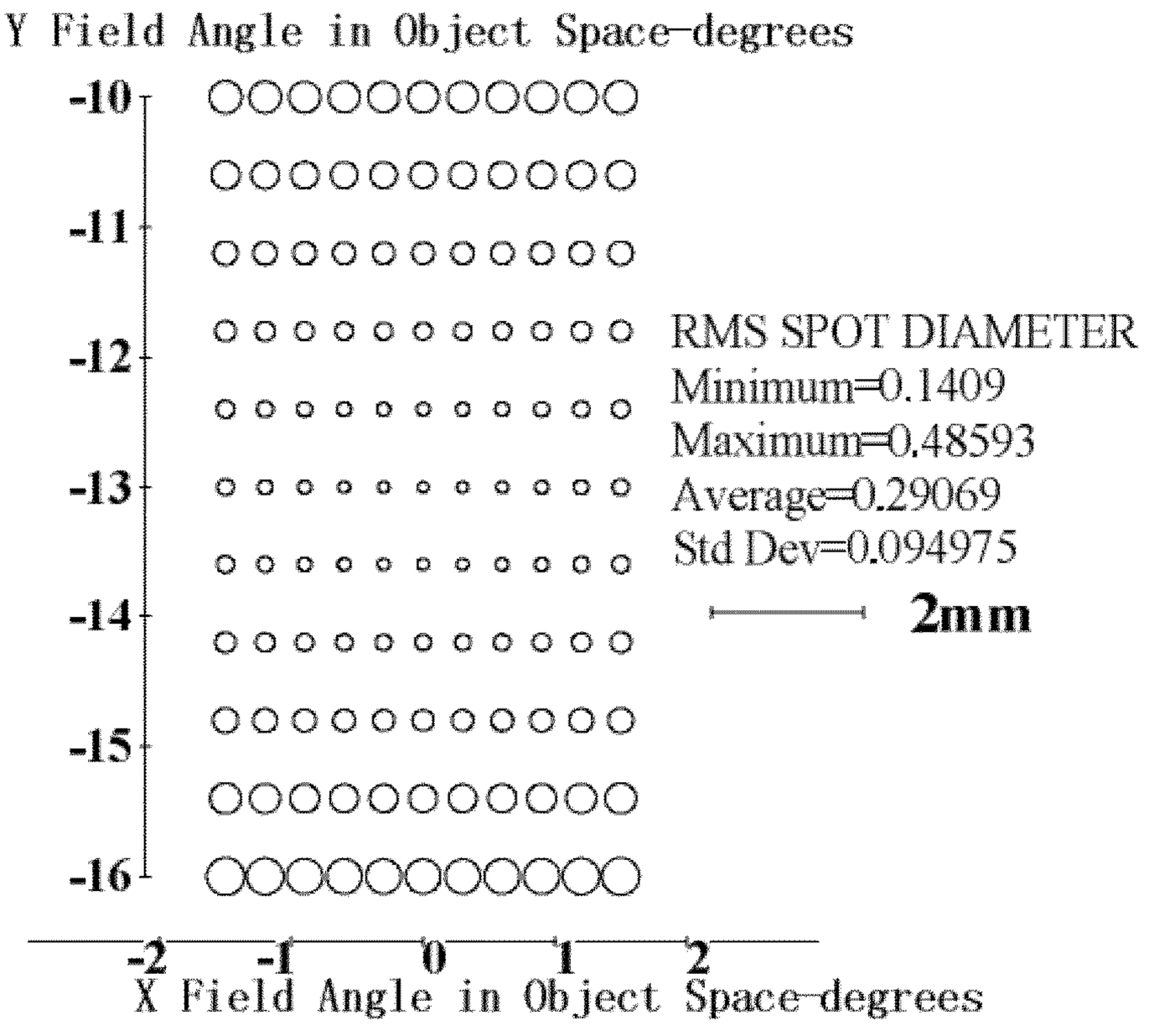

Y Field Angle in Object Space-degrees
-10
-11
-12
-13
-14
-15
-16
RMS SPOT DIAMETER
Minimum=0.1409
Maximum=0.48593
Average=0.29069
Std Dev=0.094975
2mm
-2
-1
0
1
2
X Field Angle in Object Space-degrees

FIG.9

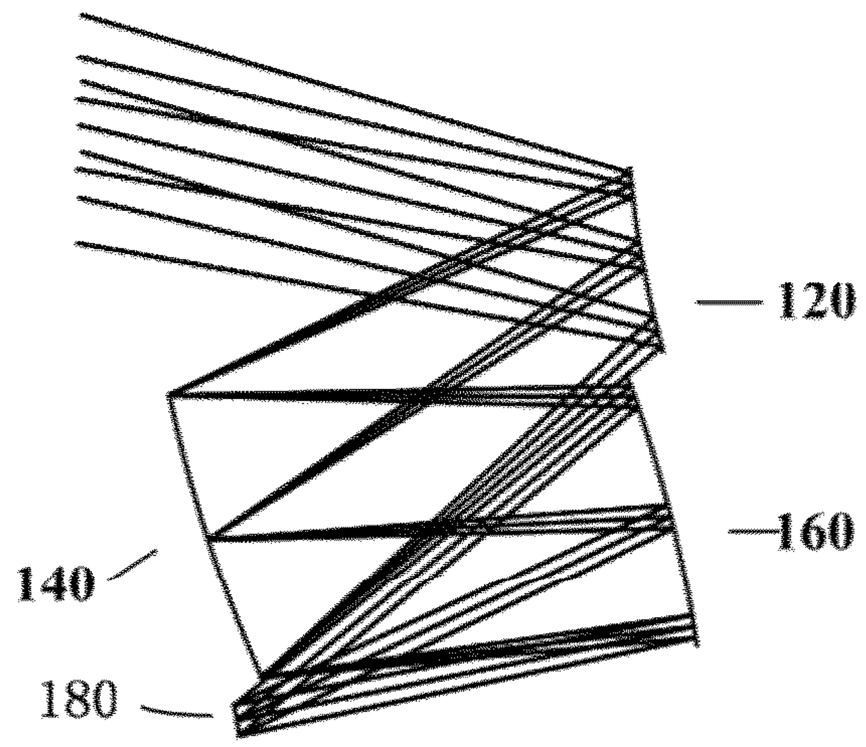


FIG.10

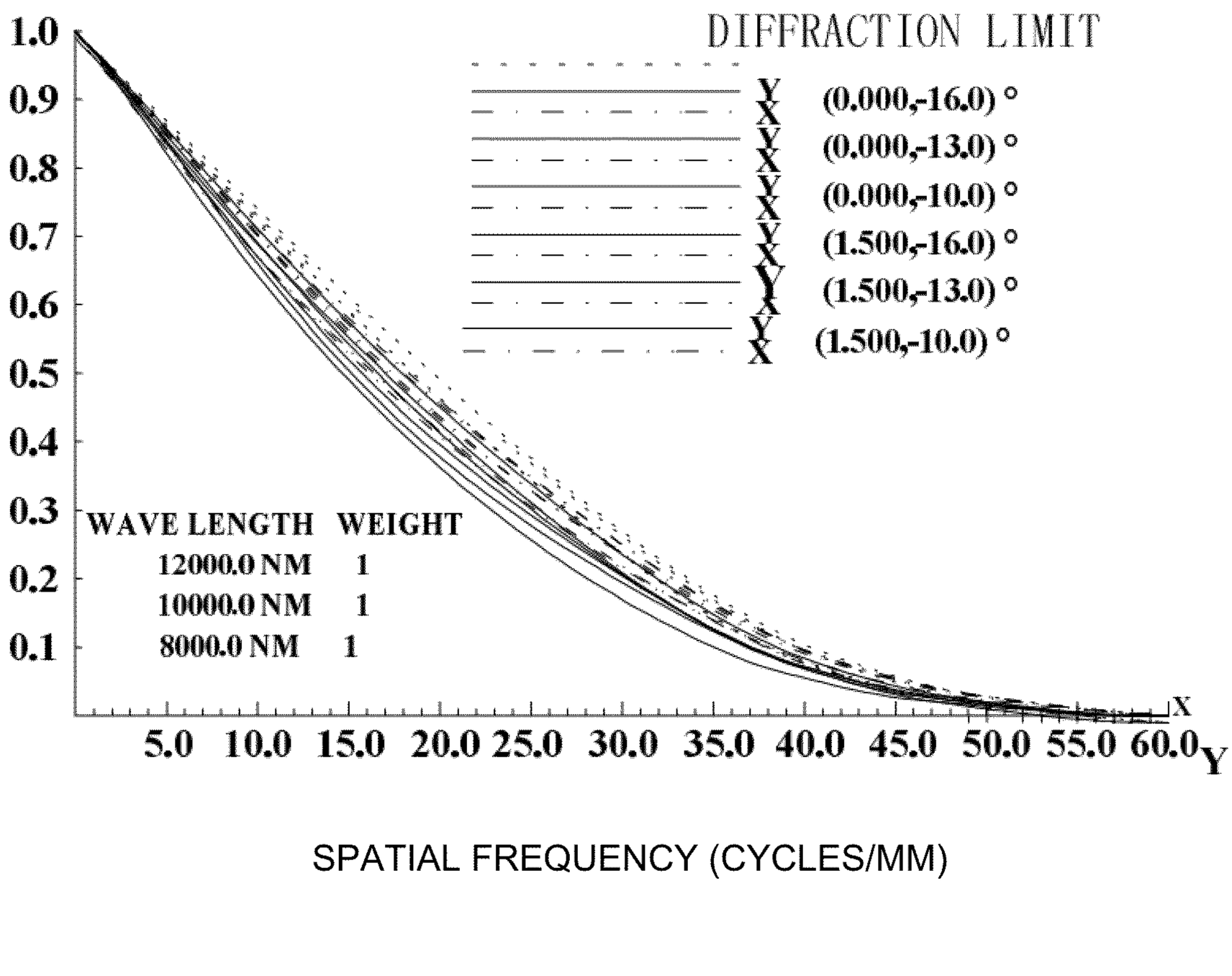

MODULATION
1.0
0.9
0.8
0.7
0.6
0.5
0.4
0.3
0.2
0.1
DIFFRACTION LIMIT
(0.000,-16.0) °
(0.000,-13.0) °
(0.000,-10.0) °
(1.500,-16.0) °
(1.500,-13.0) °
(1.500,-10.0) °
WAVE LENGTH WEIGHT
12000.0 NM 1
10000.0 NM 1
8000.0 NM 1
X
5.0 10.0 15.0 20.0 25.0 30.0 35.0 40.0 45.0 50.0 55.0 60.0
Y
SPATIAL FREQUENCY (CYCLES/MM)

FIG.11

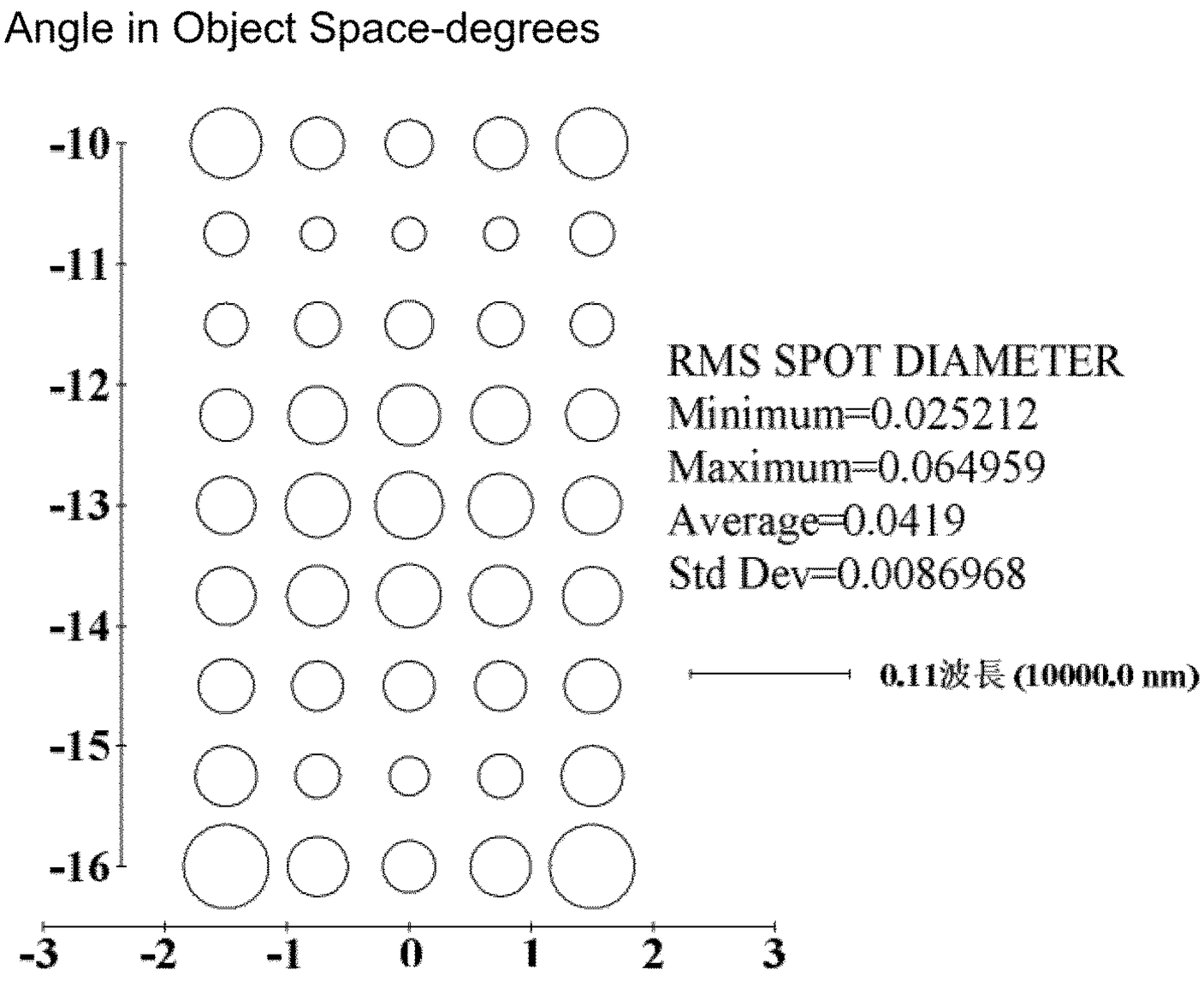

Y Field Angle in Object Space-degrees
-10
-11
-12
-13
-14
-15
-16
-3
-2
-1
0
1
2
3
RMS SPOT DIAMETER
Minimum=0.025212
Maximum=0.064959
Average=0.0419
Std Dev=0.0086968
0.11波長 (10000.0 nm)
X Field Angle in Object Space-degrees

FIG.12

OFF-AXIS HYBRID SURFACE THREE-MIRROR OPTICAL SYSTEM

CROSS-REFERENCE TO RELATED APPLICATIONS

This application claims all benefits accruing under 35 U.S.C. § 119 from China Patent Application No. 201710059417.9, field on Jan. 24, 2017 in the China Intellectual Property Office, disclosure of which is incorporated herein by reference. The application is also related to copending applications entitled, "METHOD FOR DESIGNING HYBRID SURFACE OPTICAL SYSTEM", filed Dec. 14, 2017.

FIELD

The present disclosure relates to an off-axis hybrid surface three-mirror optical system.

BACKGROUND

In a condition of meeting the optical performance requirements of an optical system, using a spherical surface or an aspheric surface to replace a freeform surface of the optical system can reduce a cost and a difficulty of processing and testing. A hybrid surface optical system comprises different surfaces. Each surface of the hybrid surface optical system can be selected from spherical surface, aspheric surface, and freeform surfaces. Thus, compared to freeform surface optical systems, the hybrid surface optical system has low cost and small processing and testing difficulty.

However, conventional off-axis hybrid surface three-mirror optical system are mainly applied to linear field of view with small field angles and large F-number, but the applications in the field of view with large field angles and small F-number are limited.

BRIEF DESCRIPTION OF THE DRAWINGS

Implementations of the present technology will now be described, by way of example only, with reference to the attached figures.

FIG. **1** is a schematic view of start point and end point of one feature ray while calculating the feature data points.

FIG. **2** is a position diagram of one embodiment of a global coordinate system and a first local coordinate system.

FIG. **3** is a schematic view of one embodiment of calculating an intermediate point G_m.

FIG. **4** is a schematic view of one embodiment of calculating a feature data point P_{m+1}.

FIG. **5** is a schematic view of one embodiment of calculating an off-axis spherical surface three-mirror optical system.

FIG. **6** is a schematic view of one embodiment of determining the parameters of the first local coordinate system.

FIG. **7** is a schematic view of one embodiment of a configuration of an off-axis hybrid surface three-mirror optical system.

FIG. **8** is a position diagram of one embodiment of a primary mirror, a secondary mirror and a tertiary mirror of an off-axis hybrid surface three-mirror optical system.

FIG. **9** shows average RMS spot diameters of one embodiment of an off-axis hybrid surface three-mirror optical system.

FIG. **10** shows a light path schematic view of one embodiment of an off-axis hybrid surface three-mirror optical system after optimization.

FIG. **11** shows a modulation transfer function (MTF) curve of one embodiment of an off-axis hybrid surface three-mirror optical system after optimization.

FIG. **12** shows a RMS wavefront error diagram of one embodiment of an off-axis hybrid surface three-mirror optical system after optimization.

DETAILED DESCRIPTION

It will be appreciated that for simplicity and clarity of illustration, where appropriate, reference numerals have been repeated among the different figures to indicate corresponding or analogous elements. In addition, numerous specific details are set forth in order to provide a thorough understanding of the embodiments described herein. However, it will be understood by those of ordinary skill in the art that the embodiments described herein can be practiced without these specific details. In other instances, methods, procedures, and components have not been described in detail so as not to obscure the related relevant feature being described. Also, the description is not to be considered as limiting the scope of the embodiments described herein. The drawings are not necessarily to scale and the proportions of certain parts have been exaggerated to better illustrate details and features of the present disclosure.

Several definitions that apply throughout this disclosure will now be presented.

The term "substantially" is defined to be essentially conforming to the particular dimension, shape, or other feature that the term modifies, such that the component need not be exact. For example, "substantially cylindrical" means that the object resembles a cylinder, but can have one or more deviations from a true cylinder. The term "comprising," when utilized, means "including, but not necessarily limited to"; it specifically indicates open-ended inclusion or membership in the so-described combination, group, series and the like.

A method for designing a hybrid surface optical system of one embodiment is provided. The method comprises the following steps:

step (**S1**), establishing a first initial system, wherein the first initial system comprises a plurality of initial surfaces, and each of the plurality of initial surfaces corresponds to a surface of an off-axis hybrid surface optical system to be calculated; and selecting a plurality of feature rays R_i (i=1, 2 . . . K) from different fields and different aperture positions;

step (**S2**), a spherical surface of the off-axis hybrid surface optical system to be calculated is defined as a spherical surface "a", keeping the plurality of initial surfaces of the first initial system unchanged and calculating a plurality of first feature data points (P_1, P_2, . . . P_m) point by point, wherein m is less than K, and the plurality of first feature data points (P_1, P_2, . . . P_m) are m intersection points of the spherical surface "a" and m of the plurality of feature rays R_1 (i=1, 2 . . . K); and surface fitting the plurality of first feature data points (P_1, P_2, . . . P_m) to obtain an initial spherical surface A_m; calculating a (m+1)th first feature data point P_{m+1} based on the initial spherical surface A_m, and surface fitting the (m+1) first feature data points (P_1, P_2, . . . P_m, P_{m+1}) to obtain a spherical surface A_{m+1}; repeating such steps until a Kth first feature data point P_K is calculated, and surface fitting the first feature data points (P_1, P_2, . . . P_K) to obtain a spherical surface A_K, wherein the spherical surface A_K is the spherical surface "a"; repeating

such steps until all spherical surfaces of the off-axis hybrid surface optical system to be calculated are obtained, to obtain a spherical surface optical system;

step (S**3**), an aspheric surface of the off-axis hybrid optical system to be calculated is defined as an aspheric surface "b", the spherical surface optical system is as a second initial system, keeping all spherical surfaces of the aspheric optical system unchanged and calculating a plurality of second feature data points (P'_1, P'_2, . . . P'_K), wherein the plurality of second feature data points (P'_1, P'_2, . . . P'_K) are the intersection points of the spherical surface "a" and the plurality of feature rays R_i (i=1, 2 . . . K); and surface fitting the plurality of second feature data points (P'_1, P'_2, . . . P'_K) to obtain the aspheric surface "b"; repeating such steps until all aspheric surfaces of the off-axis hybrid surface optical system to be calculated are obtained, to obtain a first hybrid surface optical system; and

step (S**4**), a freeform surface of the off-axis hybrid optical system to be calculated is defined as a freeform surface "c", the first hybrid surface optical system is as a third initial system, keeping all aspheric surfaces of the first hybrid surface optical system unchanged and calculating a plurality of third feature data points (P''_1, P''_2, . . . P''_K), wherein the plurality of third feature data points (P''_1, P''_2, . . . P''_K) are the intersection points of the aspheric surface "b" and the plurality of feature rays R_i (i=1, 2 . . . K); and surface fitting the plurality of third feature data points (P''_1, P''_2, . . . P''_K) to obtain the freeform surface "c"; repeating such steps until all freeform surface s of the off-axis hybrid surface optical system to be calculated are obtained.

In step (S**1**), a premise for establishing the initial system is to eliminate obscuration. The initial surface can be a planar surface or a spherical surface. In one embodiment, the initial system comprises three initial surfaces; the three initial surfaces are a primary mirror initial surface, a secondary mirror initial surface and a tertiary mirror initial surface. Each of the primary mirror initial surface, the secondary mirror initial surface and the tertiary mirror initial surface is a planar surface with eccentricity and inclination.

A method for selecting the plurality of feature rays R_i (i=1, 2 . . . K) from different fields and different aperture positions comprises steps of: M fields are selected according to the optical systems actual needs; an aperture of each of the M fields is divided into N equal parts; and, P feature rays at different aperture positions in each of the N equal parts are selected. As such, K=M×N×P different feature rays correspond to different aperture positions and different fields are fixed. The aperture can be circle, rectangle, square, oval or other shapes. In one embodiment, the aperture of each of the M fields is a circle, and a circular aperture of each of the M fields is divided into N angles with equal interval φ, as such, N=2π/φ; then, P different aperture positions are fixed along a radial direction of each of the N angles. Therefore, K=M×N×P different feature rays correspond to different aperture positions and different fields are fixed. In one embodiment, fourteen fields are fixed in the construction process, the fourteen fields are (0°, −16°), (0°, −15°), (0°, −14°), (0°, −13°), (0°, −12°), (0°, −11°), (0°, −10°), (1.5°, −16°), (1.5°, −15°), (1.5°, −14°), (1.5°, −13°), (1.5°, −12°), (1.5°, −11°), and (1.5°, −10°); one hundred and twelve feature rays are fixed from each of the fourteen fields. Therefore, 1568 different feature rays correspond to different aperture positions and different fields are fixed.

Referring to FIG. **1**, a surface Ω is defined as an unknown aspheric surface, a surface Ω' is defined as a surface located adjacent to and before the surface Ω, and a surface Ω" is defined as a surface located adjacent to and behind the surface Ω. Defining the intersection points of the plurality of feature rays R_i (i=1, 2 . . . K) with the surface Ω as the first feature data points P_i (i=1, 2 . . . K). The first feature data points P_i (i=1, 2 . . . K) can be obtained by the intersection points of the feature rays R_i (i=1, 2 . . . K) with the surface Ω' and the surface Ω". The plurality of feature rays R_i (i=1, 2 . . . K) are intersected with the surface Ω' at a plurality of start points S_i (i=1, 2 . . . K), and intersected with the surface Ω" at a plurality of end points E_i (i=1, 2 . . . K). When the surface Ω and the plurality of feature rays R_i (i=1, 2 . . . K) are determined, the plurality of start points S_i (i=1, 2 . . . K) of the feature rays R_i (i=1, 2 . . . K) can also be determined. The plurality of end points E_i (i=1, 2 . . . K) can be obtained based on the object-image relationship. Under ideal conditions, the feature rays R_i (i=1, 2 . . . K) emitted from the plurality of start points S_i (i=1, 2 . . . K) on the surface Ω'; pass through the first feature data points P_i (i=1, 2 . . . K) on the surface Ω; intersect with the surface Ω" at the plurality of end points E_i (i=1, 2 . . . K); and finally intersect with the image plane at the plurality of ideal image points I_i (i=1, 2 . . . K). When the surface Ω is a tertiary mirror, a plurality of intersection points of the plurality of feature rays R_i (i=1, 2 . . . K) and a secondary mirror are the plurality of start points S_i (i=1, 2 . . . K), a plurality of intersection points of the plurality of feature rays R_i (i=1, 2 . . . K) and the image plane are the plurality of end points E_i (i=1, 2 . . . K), and the plurality of end points E_i (i=1, 2 . . . K) are the plurality of ideal image points I_i (i=1, 2 . . . K). When the surface Ω is the secondary mirror, a plurality of intersection points of the plurality of feature rays R_i (i=1, 2 . . . K) and a primary mirror are the plurality of start points I_i (i=1, 2 . . . K), the plurality of end points E_i (i=1, 2 . . . K) are the points on the tertiary mirror which minimizes an optical path length between the plurality of first feature data points P_i (i=1, 2 . . . K) and the plurality of ideal image points I_i (i=1, 2 . . . K). When the surface Ω is the primary mirror, the plurality of end points E_i (i=1, 2 . . . K) are the points on the secondary mirror which minimizes an optical path length between the plurality of feature data points P_i (i=1, 2 . . . K) and the plurality of ideal image points I_i (i=1, 2 . . . K).

In step (S**2**), a value of m is selected to improve an accuracy of the aspheric surface fitting. In one embodiment, the value of m can be ranged from about K/3 to about 2K/3. If the value of m is too small, such as less than K/3, a surface fitting error will be large; on the contrary, if the value of m is too large, such as large than 2K/3, the subsequent feature data points are few, which is not conducive to further reduce the fitting surface error. In one embodiment, the value of m is about K/2=784.

A method for calculating the plurality of first feature data points (P_1, P_2, . . . P_m) includes the following sub-steps:

Step (a): defining a first intersection point of a first feature ray R_1 and the spherical surface "a" as the first feature data point P_1;

Step (b): when an ith (1≤i≤m−1) first feature data point P_i (1≤i≤m−1) has been obtained, a unit normal vector $\vec{N}_i$ at the ith (1≤i≤m−1) first feature data point P_i (1≤i≤m−1) can be calculated based on the vector form of Snell's Law;

Step (c): making a first tangent plane through the ith (1≤i≤m−1) first feature data point P_1 (1≤i≤m−1); and (m−i) second intersection points can be obtained by the first tangent plane intersects with remaining (m−i) feature rays; a second intersection point Q_{i+1}, which is nearest to the ith (1≤i≤m−1) feature data point P_1 (1≤i≤m−1), is fixed; and a feature ray corresponding to the second intersection point Q_{i+1} is defined as R_{i+1}, a shortest distance between the

second intersection point Q_{i+1} and the ith ($1 \le i \le m-1$) first feature data point P_i ($1 \le i \le m-1$) is defined as d_i;

Step (d): making a second tangent plane at (i-1) first feature data points that are obtained before the ith first feature data point P_i ($1 \le i \le m-1$) respectively; thus, (i−1) second tangent planes can be obtained, and (i-1) third intersection points can be obtained by the (i-1) second tangent planes intersecting with a feature ray R_{i+1}; in each of the (i-1) second tangent planes, each of the third intersection points and its corresponding feature data point form an intersection pair; the intersection pair, which has the shortest distance between a third intersection point and its corresponding feature data point, is fixed; and the third intersection point and the shortest distance is defined as Q'_{i+1} and d'_i respectively;

Step (e): comparing d_i and d'_i, if $d_i \le d'_i$, Q_{i+1} is taken as the next first feature data point P_{1+1} ($1 \le i \le m-1$); otherwise, Q'_{i+1} is taken as the next first feature data point P_{i+1} ($1 \le i \le m-1$); and

Step (f): repeating steps from b to e, until the plurality of first feature data points P_i (i=1, 2 . . . m) are all calculated.

In step (b), the unit normal vector $\vec{N}_i$ ($1 \le i \le m-1$) at each of the first feature data point P_i ($1 \le i \le m-1$) can be calculated based on the vector form of Snell's Law. When the surface Ω is a refractive surface,

$$\vec{N}_i = \frac{n'\vec{r}'_i - n\vec{r}_i}{|n'\vec{r}'_i - n\vec{r}_i|},$$

wherein

$$\vec{r}_i = \frac{\overrightarrow{P_iS_i}}{|\overrightarrow{P_iS_i}|}$$

is a unit vector along a direction of an incident ray of the surface Ω;

$$\vec{r}'_i = \frac{\overrightarrow{E_iP_i}}{|\overrightarrow{E_iP_i}|}$$

is a unit vector along a direction of an exit ray of the surface Ω; and n, n' is refractive index of a media at two opposite sides of the surface Ω respectively.

Similarly, when the surface Ω is a reflective surface,

$$\vec{N}_i = \frac{\vec{r}'_i - \vec{r}_i}{|\vec{r}'_i - \vec{r}_i|}.$$

The unit normal vector $\vec{N}_i$ at the first feature data points P_i (i=1, 2 . . . m) is perpendicular to the first tangent plane at the feature data points P_i (i=1, 2 . . . m). Thus, the first tangent planes at the first feature data points P_i (i=1, 2 . . . m) can be obtained.

Referring to FIG. **2**, a global coordinate system is defined by a primary mirror location. A beam propagation direction is defined as a Z-axis. A plane perpendicular to the Z-axis is defined as an xy plane.

Referring to FIG. **3**, during calculating the plurality of first feature data points (P_1, P_2, . . . P_m), a intermediate point G_m is calculated. A method for calculating the intermediate point G_m comprises: a tangent plane T_m at the first feature data point P_m is calculated, the tangent plane T_m intersects with the initial spherical surface A_m at an intersection line L_m; and in the global coordinate system, a first feature data point located on the intersection line L_m whose x coordinate is the same as an x coordinate of the first feature data point P_m is defined as the intermediate point G_m.

The first feature data point P_{m+1} is an intersection point between its corresponding feature ray and a tangent plane of the first feature data points (P_1, P_2, . . . P_m) that is closest to the feature data point P_{m+1}.

Referring to FIG. **4**, a method for calculating the (m+1)th first feature data point P_{m+1} comprises the sub steps: first, finding the feature ray corresponding to the (m+1)th first feature data point P_{m+1} wherein the feature ray corresponding to the (m+1)th first feature data point P_{m+1} is nearest to the intermediate point G_m in the remaining K-m characteristic rays. Since the intermediate point G_m is located on the initial spherical surface A_m, a normal vector n_m and a tangent plane of the intermediate point G_m at the initial spherical surface A_m can be obtained according to an spherical surface expression. (K-m) intersection points can be obtained by the tangent plane of the intermediate point G_m intersecting with remaining (K-m) feature rays, an intersection point O_m, which is nearest to the intermediate point G_m is fixed from the (K-m) intersection points; the feature ray where the intersection point O_m is located on is the feature ray R_{m+1} that corresponds to the feature data point P_{m+1}. Second, m intersection points O_i ($1 \le i \le m$) can be obtained by the feature ray R_{m+1} intersects with each of the tangent planes of the first feature data points (P_1, P_2 . . . P_m), and an intersection point G'_m can be obtained by the feature ray R_{m+1} intersects with the intermediate point G_m. The first feature data points (P_1, P_2 . . . P_m) and the intermediate point G_m are defined as "F"; the m intersection points O_i ($1 \le i \le m$) and the intersection point G'_m are defined as "F". A pair of (F-F') which has shortest distance is found from (P_1, P_2 . . . P_m)-O_i and G'_m-G_m. The point F is closest to the first feature data point P_{m+1}, and the point F' is the next first feature data point P_{m+1}.

The methods for calculating the first feature data points P_{m+2} and P_K are the same as the method for calculating the first feature data point P_{m+1}. A method for calculating an intermediate point G_{m+1} in a process of calculating the first feature data point P_{m+2} and a method for calculating an intermediate point G_{K-1} in a process of calculating the first feature data point P_K are the same as the method for calculating the intermediate point G_m.

A method for surface fitting the first feature data points (P_1, P_2 . . . P_m) to obtain the initial spherical surface A_m, a method for surface fitting the (m+1) first feature data points (P_1, P_2, . . . P_m, P_{m+1}) to obtain the spherical surface A_{m+1}, and a method for surface fitting the first feature data points (P_1, P_2, . . . P_K) to obtain the spherical surface A_K are all least squares method.

A coordinate of the first feature data point is (x_i, y_i, z_i), and its corresponding normal vector is (u_i, v_i, −1). When a sphere center is (A, B, C) and a radius is r, An equation of the spherical surface can be expressed by equation (1):

$$(x_i-A)^2+(y_i-B)^2+(z_i-C)^2=r^2 \quad (1).$$

Calculating a derivation of the equation (1) for x and y, to obtain an expression of a normal vector u_i in an x-axis direction and an expression of a normal vector v_i in a y-axis direction.

$$\left(1+\frac{1}{u_i^2}\right)(x_i-A)^2+(y_i-B)^2=r^2, \tag{2}$$

$$(x_i-A)^2+\left(1+\frac{1}{v_i^2}\right)(y_i-B)^2=r^2. \tag{3}$$

Equations (1) (2) and (3) can be rewrite into the matrix form, and equations (4) (5) and (6) of center coordinates can be obtained through a matrix transformation.

$$\begin{bmatrix} \sum(x_i(x_i-\bar{x})) & \sum(x_i(y_i-\bar{y})) & \sum(x_i(z_i-\bar{z})) \\ \sum(x_i(y_i-\bar{y})) & \sum(y_i(y_i-\bar{y})) & \sum(y_i(z_i-\bar{z})) \\ \sum(x_i(z_i-\bar{z})) & \sum(y_i(z_i-\bar{z})) & \sum(z_i(z_i-\bar{z})) \end{bmatrix}\begin{bmatrix} 2A \\ 2B \\ 2C \end{bmatrix}= \tag{4}$$

$$\begin{bmatrix} \sum((x_i^2+y_i^2+z_i^2)(x_i-\bar{x})) \\ \sum((x_i^2+y_i^2+z_i^2)(y_i-\bar{y})) \\ \sum((x_i^2+y_i^2+z_i^2)(z_i-\bar{z})) \end{bmatrix},$$

$$\begin{bmatrix} \sum U_i(U_i-\bar{U}) & \sum U_i(y_i-\bar{y}) & 0 \\ \sum U_i(y_i-\bar{y}) & \sum y_i(y_i-\bar{y}) & 0 \\ 0 & 0 & 0 \end{bmatrix}\begin{bmatrix} 2A \\ 2B \\ 2C \end{bmatrix}= \tag{5}$$

$$\begin{bmatrix} \sum(U_ix_i+y_i^2)(U_i-\bar{U}) \\ \sum(U_ix_i+y_i^2)(y_i-\bar{y}) \\ 0 \end{bmatrix},$$

$$\begin{bmatrix} \sum x_i(x_i-\bar{x}) & \sum V_i(x_i-\bar{x}) & 0 \\ \sum V_i(x_i-\bar{x}) & \sum V_i(V_i-\bar{V}) & 0 \\ 0 & 0 & 0 \end{bmatrix}\begin{bmatrix} 2A \\ 2B \\ 2C \end{bmatrix}=\begin{bmatrix} \sum(x_i^2+V_iy_i)(x_i-\bar{x}) \\ \sum(x_i^2+V_iy_i)(V_i-\bar{V}) \\ 0 \end{bmatrix}. \tag{6}$$

The normal vector (u_i, v_i, −1) decides a direction of light rays, thus, both a coordinate error and a normal error during the surface fitting should be considered to obtain an accurate spherical surface. The coordinate error and the normal error are linearly weighted to solve the sphere center (A, B, C) and the radius r.

$$\text{Equation (4)}+\omega\times\text{equation (5)}+\omega\times\text{equation (6)} \tag{7},$$

$$\text{Equation (1)}+\omega\times\text{equation (2)}+\omega\times\text{equation (3)} \tag{8},$$

wherein, ω is a weight of the normal error. The sphere center (A, B, C) can be obtained by equation (7), and the radius r can be obtained by equation (8).

After the spherical surface "a" is obtained, the radius of the spherical surface "a" can be further changed to obtain a spherical surface "a'", an optical power of the spherical surface "a" is changed. In one embodiment, $r_a'=\varepsilon_a\times r_a$, $\varepsilon_a=0.5\sim1.5$, wherein, r_a is the radius of the spherical surface "a", and r_a' is the radius of the spherical surface "a'". The radius of each of the spherical surfaces of the off-axis hybrid surface optical system can be further changed to change the optical power each of the spherical surfaces. Referring to FIG. **5**, in one embodiment, a spherical surface "C" is obtained by the method like in step S**2**, a spherical surface "C'" is obtained by changing a radius of the spherical surface "C"; the primary mirror initial plane and the spherical surface "C'" are kept unchanged to solve a spherical surface "B", and a spherical surface "B'" is obtained by changing a radius of the spherical surface "B"; the spherical surface "B'" and the spherical surface "C'" are kept unchanged to solve a spherical surface "A", and a spherical surface "A'" is obtained by changing a radius of the spherical surface "A", therefore, a spherical three-mirror optical system comprising the spherical surface "A'", the spherical surface "B'" and the spherical surface "C'" is obtained.

In step (S**3**), the normal vector N=(U,V,−1) determines a deflection direction of light rays. If a normal surface fitting error is large, a propagation path of the feature ray will deviate from an expected direction. Therefore, both a coordinate error and a normal error during the surface fitting the plurality of second feature data points (P'_1, P'_2, P'_K) should be considered. A unit normal vector of each of the plurality of second feature data points (P'_1, P'_2, P'_K) is obtained based on the object-image relationship, and the coordinates and normal of the K second feature data points are surface fitted.

A method for calculating the unit normal vector at each of the second feature data points is the same as the method for calculating the unit normal vector at each of the first feature data points.

A first local coordinate system is defined with a center of the aspheric surface (0, a', b') as an origin and an aspherical symmetry axis as a Z-axis. The first local coordinate system xyz can be described by the parameters (a, b, θ), wherein θ is a rotation angle of the first local coordinate system relative to the global coordinate system.

The coordinate error and the normal error are linearly weighted, and an error evaluation function J is proposed:

$$\begin{aligned} J&=\sum(Z-z)^2+\omega\times\sum(U-u)^2+\omega\times\sum(V-v)^2 \\ &=(z-A_1P)^T(z-A_1P)+\omega(u-A_2P)^T(v-A_2P)+ \\ &\quad\omega(v-A_3P)^T(v-A_3P), \end{aligned} \tag{10}$$

wherein Z is a surface fitting coordinate, (U, V, −1) is the surface fitting normal vector, z is a real coordinate, (u, v, −1) is a real normal vector, ω is a weight of the normal error, P is an coefficient matrix (A, B, C, D . . .) of the aspheric surface "b", A_1 is a matrix (r^2, r^4, r^6, r^8 . . .), A_2 is a matrix obtained by calculating the partial derivatives of A_1 with respect to x, and A_3 is a matrix obtained by calculating the partial derivatives of A_1 with respect toy.

When the error evaluation function J is smallest, a calculating equation of the coefficient matrix P is:

$$P=(A_1^TA_1+\omega A_2^TA_2+\omega A_3^TA_3)^{-1}(A_1^Tz+\omega A_2^Tu+\omega A_3^Tv) \tag{11}.$$

A method for surface fitting the second feature data points (P'_1, P'_2, . . . P'_K) to obtain the aspheric surface "b" comprising the sub-step:

step (S**31**), transferring the coordinates (x_0, y_0, z_0) of the second feature data points (P'_1, P'_2, . . . P'_K) and their corresponding normal vectors (α_0, β_0, γ_0) in the global coordinate system to the coordinates (x, y, z) and their corresponding normal vectors (α, β, γ) in the first local coordinate system; and

step (S**32**), performing the least squares fitting in the first local coordinate system xyz.

In step (S**31**), a relationship between the coordinates (x_0, y_0, z_0) in the global coordinate system $x_0y_0z_0$ and the coordinates (x, y, z) in the first local coordinate system xyz can be written as:

$$\begin{cases} x=x_0 \\ y=(y_0-a)\cos\theta-(z_0-b)\sin\theta \\ z=(y_0-a)\sin\theta+(z_0-b)\cos\theta \end{cases}.$$

A relationship between the normal vectors (α_0, β_0, γ_0) in the global coordinate system and normal vectors (α, β, γ) in the first local coordinate system xyz can be written as:

$$\begin{cases} u = u_0 \\ v = v_0\cos\theta - w_0\sin\theta \\ w = v_0\sin\theta + w_0\cos\theta \end{cases}.$$

In one embodiment, a number of the first local coordinate system positions are obtained by using a local search algorithm near the second feature data points, from which a first local coordinate system with the smallest surface fitting error is chosen, and a z-axis of the first local coordinate system with the smallest surface fitting error is as a symmetry axis of the aspheric surface "b".

Referring to FIG. **6**, a value of the aspheric vertex coordinates (0, a', b') is obtained by using a local search algorithm in a rectangle with a diagonal of the connection between the second feature data points P'_1 and P'_k. In one embodiment, a grid mesh is generated in the rectangle with the diagonal of the connection between the second feature data points P'_1 and P'_k, a grid node is a value of the vertex coordinates (0, a', b') of the aspheric surface "b", and a grid size is a step size of (0, a', b'). In one embodiment, the step size of (0, a', b') is about 0.2 mm. A value of the rotation angle θ can be ranged from about $-\pi$ to about π for each set of (a', b'). Therefore, a plurality of parameters (a', b', θ) correspond to a plurality of first local coordinate system positions can be obtained.

For each of the plurality of parameters (a', b', θ), the coefficient matrix P (A, B, C, D . . .) can be obtained by equation (11), and its corresponding J is known by equation (10). Selecting a parameter (a', b', θ) whose corresponding J is the smallest and defining it as an optimal local coordinate position parameter, and the first local coordinate system is established using the optimal local coordinate position parameter.

The coefficient matrix P (A, B, C, D . . .) is substituted into the following equation (12) to obtain the aspheric surface "b",

$$Z = Ar^2 + Br^4 + Cr^6 + Dr^8 + \ldots \quad r^2 = x^2 + y^2 \tag{12}$$

$$A = \frac{1}{2}c,\ B = a_1 + \frac{1}{8}(k+1)c^3,\ C = a_2 + \frac{1}{16}(k+1)^2c^5,$$

$$D = a_3 + \frac{5}{128}(k+1)^3c^7,$$

wherein, L is a more than eighth order term about r. Since an order of L term is too high, a processing of the aspheric surface "b" is more difficult, so the L item can be directly omitted in the actual calculation.

In step (S**4**), both a coordinate error and a normal error during surface fitting the plurality of third feature data points (P''_1, P''_2, . . . P''_K) should be considered. A unit normal vector of each of the plurality of third feature data points (P''_1, P''_2, . . . P''_K) is obtained based on the object-image relationship, and the coordinates and normal of the K third feature data points are surface fitted.

A method for calculating the unit normal vector at each of the third feature data points is the same as the method for calculating the unit normal vector at each of the first feature data points.

A method for surface fitting the plurality of third feature data points (P''_1, P''_2, . . . P''_K) to obtain the freeform surface "c" comprising the sub-step:

step (S**41**), surface fitting the plurality of third feature data points to a sphere in the global coordinate system, and obtaining a curvature c of the sphere and a curvature center (x_c, y_c, z_c) corresponding to the curvature c of the sphere;

step (S**42**), defining a feature data point (x_o, y_o, z_o) corresponding to a chief ray of the central field angle among the entire field-of-view (FOV) as the vertex of the sphere, defining a second local coordinate system by the vertex of the sphere as origin and a line passing through the curvature center and the vertex of the sphere as a Z-axis;

step (S**43**), transforming the coordinates (x_i, y_i, z_i) and the normal vector (α_i, β_i, γ_i), of the plurality of third feature data points in the global coordinate system, into the coordinates (x'_i, y'_i, z'_i) and the normal vector (α'_i, β'_i, γ'_i), of the plurality of third feature data points in the second local coordinate system;

step (S**44**), surface fitting the plurality of third feature data points into the conic surface in the second local coordinate system, based on the coordinates (x'_i, y'_i, z'_i) and the curvature c of the sphere, and obtaining the conic constant k; and

step (S**45**), removing the coordinates and the normal vector of the plurality of third feature data points P_i (i=1, 2 . . . K), on the conic surface in the second local coordinate system, from the coordinates (x'_i, y'_i, z'_i) and the normal vector (α'_i, β'_i, γ'_i), to obtain a residual coordinate and a residual normal vector; and surface fitting the residual coordinate and the residual normal vector to obtain a freeform surface; the equation of the freeform surface "c" can be obtained by adding an conic surface equation and an freeform surface equation.

Generally, the optical systems are symmetric about the yoz plane. Therefore, a tilt angle θ of the sphere, in the yoz plane of the second local coordinate system relative to in the yoz plane of the global coordinate system, is:

$$\theta = \arctan\left(\frac{y_o - y_c}{z_o - z_c}\right).$$

A relationship between the coordinates (x'_i, y'_i, z'_i) and the coordinates (x_i, y_i, z_i) of each of the plurality of third feature data points can be expressed as following:

$$\begin{cases} x'_i = x_i - x_o \\ y'_i = (y_i - y_o)\cos\theta - (z_i - z_o)\sin\theta \\ z'_i = (y_i - y_o)\sin\theta + (z_i - z_o)\cos\theta \end{cases}.$$

A relationship between the normal vector (α'_i, β'_i, γ'_i) and the normal vector (α_i, β_i, γ_i) of each of the plurality of third feature data points can be expressed as following:

$$\begin{cases} \alpha'_i = \alpha_i \\ \beta'_i = \beta_i\cos\theta - \gamma_i\sin\theta \\ \gamma'_i = \beta_i\sin\theta + \gamma_i\cos\theta \end{cases}.$$

In the second local coordinate system, the coordinates and the normal vector of the plurality of third feature data points on the conic surface are defined as (x'_i, y'_i, z'_{is}) and (α'_{is}, β'_{is}, γ'_{is}) respectively. An Z'-axis component of the normal vector

is normalized to −1. The residual coordinate (x''_i, y''_i, z''_i) and the residual normal vector (α''_i, β''_i, −1) can be obtained, wherein, (x_i'',y_i'',z_i'')=(x_i',y_i',z_i'') and

$$(\alpha_i'', \beta_i'', -1) = \left(-\frac{\alpha_i'}{\gamma_i'} + \frac{\alpha_{is}'}{\gamma_{is}'}, -\frac{\beta_i'}{\gamma_i'} + \frac{\beta_{is}'}{\gamma_{is}'}, -1\right).$$

In step (S**45**), a method of surface fitting the residual coordinate and the residual normal vector comprises:

step (S**451**): in the second local coordinate system, expressing a polynomial surface by the polynomial surface equation leaving out the conic surface term, the polynomial surface can be expressed in terms of the following equation:

$$z = f(x, y; P) = \sum_{j=1}^{J} P_j g_j(x, y),$$

wherein $g_j(x, y)$ is one item of the polynomial, and $P=(p_1, p_2, \ldots, p_J)^T$ is the coefficient sets;

step (S**452**): acquiring a first sum of squares $d_1(P)$, of residual coordinate differences in z' direction between the residual coordinate value (x''_i, y''_i, z''_i) (i=1, 2, . . . , K) and the freeform surface; and a second sum of squares $d_2(P)$, of modulus of vector differences between the residual normal vector $N_i=(\alpha''_i, \beta''_i, -1)$ (i=1, 2, . . . , K) and a normal vector of the freeform surface, wherein the first sum of squares $d_1(P)$ is expressed in terms of a first equation:

$$d_1(P) = \sum_{i=1}^{I} [z_i - f(x_i'', y_i''; P)]^2 = (Z - A_1 P)^T (Z - A_1 P),$$

and

the second sum of squares $d_2(P)$ is expressed in terms of a second equation:

$$d_2(P) = \sum_{i=1}^{I} \{[u_i - f_{x''}(x_i'', y_i''; P)]^2 + [v_i - f_{y''}(x_i'', y_i''; P)]^2\} = (U - A_2 P)^T (U - A_2 P) + (V - A_3 P)^T (V - A_3 P);$$

wherein,

$$Z = (z_1, z_2, \ldots, z_I)^T,$$

$$U = (u_1, u_2, \ldots, u_I)^T,$$

$$V = (v_1, v_2, \ldots, v_I)^T,$$

$$A_1 = \begin{pmatrix} g_1(x_1'', y_1'') & g_2(x_1'', y_1'') & \ldots & g_J(x_1'', y_1'') \\ g_1(x_2'', y_2'') & g_2(x_2'', y_2'') & \ldots & g_J(x_2'', y_2'') \\ \vdots & \vdots & & \vdots \\ g_1(x_I'', y_I'') & g_2(x_I'', y_I'') & \ldots & g_J(x_I'', y_I'') \end{pmatrix},$$

$$A_2 = \begin{pmatrix} g_1^x(x_1'', y_1'') & g_2^x(x_1'', y_1'') & \ldots & g_J^x(x_1'', y_1'') \\ g_1^x(x_2'', y_2'') & g_2^x(x_2'', y_2'') & \ldots & g_J^x(x_2'', y_2'') \\ \vdots & \vdots & & \vdots \\ g_1^x(x_I'', y_I'') & g_2^x(x_I'', y_I'') & \ldots & g_J^x(x_I'', y_I'') \end{pmatrix},$$

-continued

$$A_3 = \begin{pmatrix} g_1^y(x_1'', y_1'') & g_2^y(x_1'', y_1'') & \ldots & g_J^y(x_1'', y_1'') \\ g_1^y(x_2'', y_2'') & g_2^y(x_2'', y_2'') & \ldots & g_J^y(x_2'', y_2'') \\ \vdots & \vdots & & \vdots \\ g_1^y(x_I'', y_I'') & g_2^y(x_I'', y_I'') & \ldots & g_J^y(x_I'', y_I'') \end{pmatrix};$$

step (S**453**): obtaining an evaluation function,

$$P=(A_1{}^T A_1+wA_2{}^T A_2+wA_3{}^T A_3)^{-1}\cdot(A_1{}^T Z+wA_2{}^T U+wA_3{}^T V),$$

wherein w is a weighting greater than 0;

step (S**454**): selecting different weightings w and setting a gradient ∇f(P) of the evaluation function equal to 0, to obtain a plurality of different values of P and a plurality of freeform surface shapes z=f (x, y; P) corresponding to each of the plurality of different values of P; and

step (S**455**): choosing a final freeform surface shape Ω_{opt} which has a best imaging quality from the plurality of freeform surface shapes z=f (x, y; P).

Furthermore, a step of optimizing the hybrid surface optical system obtained after step (S**4**) can be performed, and the hybrid surface optical system obtained after step (S**4**) can be as the initial system.

Referring to FIG. **7**, an off-axis hybrid surface three-mirror optical system **100** is designed with the above method to prove the above method. The off-axis hybrid surface three-mirror optical system **100** comprises a primary mirror **120**, a secondary mirror **140**, a tertiary mirror **160** and an image sensor **180** located in that order and spaced from each other. The secondary mirror **140** is used as a stop surface. A surface shape of the primary mirror **120** is a freeform surface. A surface shape of the secondary mirror **140** is an aspheric surface. A surface shape of the tertiary mirror **160** is a spherical surface. The feature rays exiting from the light source would be successively reflected by the primary mirror **120**, the secondary mirror **140** and the tertiary mirror **160** to form an image on the image sensor **180**. The parameters of the off-axis hybrid surface three-mirror optical system **100** are shown in table 1 below.

TABLE 1

Parameters	Values
Field of View	3° × 6° (an angle in a meridian direction is in a range from −16° to −10°)
F-number	2.2
entrance pupil diameter	100 mm
Wave Range	Long-wave infrared (8-12 μm)

In one embodiment, fourteen off-axial fields are selected during a designing process of the off-axis hybrid surface three-mirror optical system **100**. The fourteen off-axial fields are (0°, −16°), (0°, −15°), (0°, −14°), (0°, −13°), (0°, −12°), (0°, −11°), (0°, −10°), (1.5°, −16°), (1.5°, −15°), (1.5°, −14°), (1.5°, −13°), (1.5°, −12°), (1.5°, −11°), and (1.5°, −10°). 112 feature rays are selected in each off-axial field, and 1568 feature rays that corresponds different pupil positions and different off-axial fields are selected.

Referring to FIG. **8**, a first three-dimensional rectangular coordinates system (x_1, y_1, z_1) is defined in space. A z_1-axis is along an horizontal line, in the z_1-axis, to the left is negative, and to the right is positive. A y_1-axis is in a direction substantially perpendicular to the z_1-axis, in the y_1-axis, to the upward is positive, and to the downward is negative. An x_1-axis is perpendicular to a y_1z_1 plane, in the

x_1-axis, in a direction substantially perpendicular to the y_1z_1 plane, to the inside is positive, and to the outside is negative.

In space relative to the first three-dimensional rectangular coordinates system (x_1, y_1, z_1), a second three-dimensional rectangular coordinates system (x_2, y_2, z_2) is defined by a primary mirror location, a third three-dimensional rectangular coordinates system (x_3, y_3, z_3) is defined by a secondary mirror location, a fourth three-dimensional rectangular coordinates system (x_4, y_4, z_4) is defined by a tertiary mirror location, and a fifth three-dimensional rectangular coordinates system (x_5, y_5 z_5) is defined by an image sensor location.

A second origin of the second three-dimensional rectangular coordinates system (x_2, y_2, z_2) in the first three-dimensional rectangular coordinates system (x_1, y_1, z_1) is (0, 244.51, 193.62), whose unit is millimeter. A z_2-axis positive direction rotates about 13.39 degrees along a counterclockwise direction relative to a z_1-axis positive direction.

A third origin of the third three-dimensional rectangular coordinates system (x_3, y_3, z_3) in the first three-dimensional rectangular coordinates system (x_1, y_1, z_1) is (0, 0, −100), whose unit is millimeter. A z_3-axis positive direction rotates about 15 degrees along a counterclockwise direction relative to a z_1-axis positive direction.

A fourth origin of the fourth three-dimensional rectangular coordinates system (x_4, y_4, z_4) in the first three-dimensional rectangular coordinates system (x_1, y_1, z_1) is (0, −160.83, 209.49), whose unit is millimeter. A z_4-axis positive direction rotates about 0 degrees along a counterclockwise direction relative to a z_1-axis positive direction.

A fifth origin of the fifth three-dimensional rectangular coordinates system (x_5, y_5, z_5) in the first three-dimensional rectangular coordinates system (x_1, y_1, z_1) is (0, −145.13, −174.41), whose unit is millimeter. A z_5-axis positive direction rotates about 10 degrees along a counterclockwise direction relative to a z_1-axis positive direction.

A length of the off-axis hybrid surface three-mirror optical system **100** along the y_1-axis is about 430 millimeters. A length of the off-axis hybrid surface three-mirror optical system **100** along the z_1-axis is about 400 millimeters.

In the second three-dimensional rectangular coordinates system (x_2, y_2, z_2); a reflective surface of the primary mirror **120** is a sixth-order polynomial freeform surface of x_2y_2, and the sixth-order polynomial freeform surface of x_2y_2 can be expressed as follows:

$$Z = \frac{cr^2}{1+\sqrt{1-(1+k)c^2r^2}} + b_1y + b_2x^2 + b_3y^2 + b_4x^2y + b_5y^3 + b_6x^4 + b_7x^2y^2 + b_8y^4 + b_9x^6 + b_{10}x^4y^2 + b_{11}x^2y^4 + b_{12}y^6$$
$$r^2 = x^2 + y^2,$$

wherein, z represents surface sag, c represents surface curvature, k represents conic constant, while b_i (i=1, 2, . . . , 11, 12) represents the ith term coefficient. In one embodiment, c=4.57e−04, k=0.048, b_1=0.0951, b_2=5.26e−06, b_3=7.90e−05, b_4=3.41e−07, b_5=3.97e−07, b_6=5.54e−10, b_7=1.29e−09, b_8=6.84e−10, b_9=0, b_{10}=0, b_{12}=0.

In the third three-dimensional rectangular coordinates system (x_3, y_3, z_3), the reflective surface of the secondary mirror **104** is a sixth-order polynomial aspheric surface of x_3y_3. The sixth-order polynomial aspheric surface of x_3y_3 can be expressed as follows:

$$Z = \frac{cr^2}{1+\sqrt{1-(1+k)c^2r^2}} + a_1r^4 + a_2r^6 \quad r^2 = x^2 + y^2,$$

wherein z represents surface sag, c represents surface curvature, k represents conic constant, a1 and a2 are polynomial coefficients. In one embodiment, c=5.73e−04,k=0, a_1=1.21e−12, a_2=−8.85e−16.

In the fourth three-dimensional rectangular coordinates system (x_4, y_4, z_4), the reflective surface of the tertiary mirror **106** is a spherical surface of x_4y_4, and the spherical surface of x_4y_4 can be expressed as $(x-A)^2+(y-B)^2+(z-C)^2=r^2$. In one embodiment, A=0, B=−160.83, C=209.49, r=−988.48.

In other embodiments, the values of c, k, and A, in the sixth-order polynomial freeform surface of x_2y_2, the values of z, c, k, a_1 and a_2 of sixth-order polynomial aspheric surface of x_3y_3, and the values of A, B, C and r of the spherical surface of x_4y_4 can be selected according to actual needs.

Referring to FIG. **9**, the RMS spot diameters of the off-axis hybrid surface three-mirror optical system **100** is shown. It can be seen that an average value of the RMS spot diameters is about 0.296 mm. It shows that the RMS spot diameters of the off-axis hybrid surface three-mirror optical system **100** is small, therefore the off-axis hybrid surface three-mirror optical system **100** can be used as a good initial structure for subsequent optimization.

The off-axis hybrid surface three-mirror optical system **100** can be optimized to improve the imaging quality and reduce the relative distortion. The off-axis hybrid surface three-mirror optical system is used as the initial structure for subsequent optimization. In one embodiment, the off-axis hybrid surface three-mirror optical system **100** is optimized via a CODEV software. In one embodiment, after the off-axis hybrid surface three-mirror optical system **100** is optimized, in the sixth-order polynomial freeform surface of x_2y_2, c=5.54e−04, k=90.31, b_1=0, b_2=0.0003, b_3=0.0005, b_4=9.07e−07, b_5=1.03e−06, b_6=−2.37e−10, b_7=9.88e−10, b_8=1.31e−09, b_9=−4.64e−14, b_{10}=−1.91e−13, b_{11}=−2.05e−13 b_{12}=−7.56e−14; in the sixth-order polynomial aspheric surface of x_3y_3, c=9.19e−04, k=0, a_1=−4.49e−11, a_2=−1.35e−15; in the spherical surface of x_4y_4, A=0, B=−266.75, C=313.84, r=−996.65.

In one embodiment, after the off-axis hybrid surface three-mirror optical system **100** is optimized, the second origin of the second three-dimensional rectangular coordinates system (x_2, y_2, z_2) is in (0, 18.57, 274.09) position of the first three-dimensional rectangular coordinates system (x_1, y_1, z_1), whose unit is millimeter. A z_2-axis positive direction rotates about 7.63 degrees along a counterclockwise direction relative to a z_1-axis positive direction. A third origin of the third three-dimensional rectangular coordinates system (x_3, y_3, z_3) is in (0, −227.00, −48.81) position of the first three-dimensional rectangular coordinates system (x_1, y_1, z_1), whose unit is millimeter. A z_3-axis positive direction rotates about 18.03 degrees along a counterclockwise direction relative to a z_1-axis positive direction. A fourth origin of the fourth three-dimensional rectangular coordinates system (x_4, y_4, z_4) is in (0, −266.75, 313.84) position of the first three-dimensional rectangular coordinates system (x_1, y_1, z_1), whose unit is millimeter. A z_4-axis positive direction rotates about 10.77 degrees along a counterclockwise direction relative to a z_1-axis positive direction. A fifth origin of the fifth three-dimensional rectangular coordinates system (x_5, y_5, z_5) is in (0, −365.47, −27.10) position of the first

three-dimensional rectangular coordinates system (x_1, y_1, z_1), whose unit is millimeter. A z_5-axis positive direction rotates about 9.74 degrees along a counterclockwise direction relative to a z_1-axis positive direction.

Referring to FIG. **10**, a light path schematic view of the off-axis hybrid surface three-mirror optical system **100** after optimization is shown. It is shown that the plurality of feature rays R_i (i=1, 2 . . . K) from different fields and different aperture positions substantially focus on the ideal target point, the image quality is improved.

FIG. **11** illustrates that a modulation transfer functions (MTF) in visible light band of partial field angles of the hybrid surface three-mirror optical system **100** after optimization are closes to the diffraction limitation, and the image quality is further improved.

Referring to FIG. **12**, it can be seen that the average root mean square (RMS) of the pixel spot of the hybrid surface three-mirror optical system **100** after optimization is about 0.042λ, wherein λ=10000 nm, which meets the design requirements.

An effective entrance pupil diameter of the hybrid surface three-mirror optical system **100** is about 100 millimeter.

The hybrid surface three-mirror optical system **100** adopts an off-axis field of view in a vertical direction. A field angle of the hybrid surface three-mirror optical system **100** is about 3°×6°, wherein an angle in an horizontal direction is in a range from about −1.5° to about 1.5°, and an angle in the vertical direction is in a range from about −16° to about −10°.

A wavelength of the hybrid surface three-mirror optical system **100** is not limited, in one embodiment, the wavelength is in a range from about 8 microns to about 12 microns.

An effective focal length (EFL) of the hybrid surface three-mirror optical system **100** is about 220 millimeters.

F-number of the hybrid surface three-mirror optical system **100** is a D/f reciprocal. In one embodiment, the relative aperture (D/f) of the hybrid surface three-mirror optical system **100** is about 0.45, and the F-number is about 2.2.

The method for designing hybrid surface three-mirror optical system can have many advantages. First, the method is calculated directly in an off-axis state, an error produced during a process from the coaxial system transformed into the off-axis system can be avoided, thus, a deviation between the off-axis hybrid surface optical system obtained by the above method and an ideal optical system is small. Second, during calculating the spherical surface optical system, the surface fitting process is combined with the data point calculating process, the unknown surface is calculated by repeating the process of data point calculating-spherical surface fitting, which improve the accuracy of the method. Third, the optical power of the spherical surface is changed by changing the radius of the spherical surface, then the remaining spherical surface is calculated to compensate for changed optical power. Therefore, an optical power distribution of the spherical surface optical system is more uniform, and the spherical surface optical system can be a better initial system for the following steps. Fourth, the global coordinate system and the local coordinate system are defined, the coordinates and the normal vector of the plurality of feature data points in the global coordinate system are transformed into the local coordinate system, then the aspheric surfaces are obtained by surface fitting in the local coordinate system, thus, the method is more precisely compared to conventional methods. Fifth, when surface fitting the second plurality of feature data points and the third plurality of feature data points, both the coordinates and the normal vectors of the second plurality of feature data points and the third plurality of feature data points are considered; therefore, the shape of the freeform surface and shape of the aspheric surfaces are accurate. Finally, the point-by-point design method can be used to design hybrid surface systems comprise different surfaces, increasing the diversity of optical designs.

It is to be understood that the above-described embodiments are intended to illustrate rather than limit the present disclosure. Variations may be made to the embodiments without departing from the spirit of the present disclosure as claimed. Elements associated with any of the above embodiments are envisioned to be associated with any other embodiments. The above-described embodiments illustrate the scope of the present disclosure but do not restrict the scope of the present disclosure.

What is claimed is:

1. An off-axis hybrid surface three-mirror optical system comprising:

a primary mirror located on an outgoing light path of rays;

a secondary mirror located on a first reflected light path, which is emitted from the primary mirror;

a tertiary mirror located on a second reflected light path, which is emitted from the secondary mirror; and

an image sensor located on a third reflected light path, which is emitted from the tertiary mirror;

wherein a first three-dimensional rectangular coordinates system (x_1 y_1, z_1) is defined in space; relative to the first three-dimensional rectangular coordinates system (x_1, y_1, z_1), a second three-dimensional rectangular coordinates system (x_2 y_2 z_2) is defined by a primary mirror location, a third three-dimensional rectangular coordinates system (x_3, y_3, z_3) is defined by a secondary mirror location, and a fourth three-dimensional rectangular coordinates system (x_4 y_4, z_4) is defined by a tertiary mirror location; in the second three-dimensional rectangular coordinates system (x_2, y_2, z_2), a reflective surface of the primary mirror is a sixth-order polynomial freeform surface of x_2y_2; in the third three-dimensional rectangular coordinates system (x_3, y_3, z_3), a reflective surface of the secondary mirror is a sixth-order polynomial aspheric surface of x_3y_3, and the sixth-order polynomial aspheric surface of x_3 y_3 is:

$$Z = \frac{cr^2}{1+\sqrt{1-(1+k)c^2r^2}} + a_1r^4 + a_2r^6 \quad r^2 = x^2 + y^2,$$

wherein z represents surface sag, c represents surface curvature, k represents conic constant, a_1 and a_2 are polynomial coefficients, c=5.73e−04, k=0, a_1=1.21e−12, and a_2=−8.85e−16; and in the fourth three-dimensional rectangular coordinates system (x_4, y_4, z_4), a reflective surface of the a tertiary mirror is a spherical surface of x_4y_4.

2. The system as claimed in claim **1**, wherein a second origin of the second three-dimensional rectangular coordinates system (x_2, y_2, z_2) in the first three-dimensional rectangular coordinates system (x_1, y_1, z_1) is (0, 244.51, 193.62).

3. The system as claimed in claim **2**, wherein an z_2-axis positive direction rotates about 13.39 degrees along a counterclockwise direction relative to an z_1-axis positive direction.

4. The system as claimed in claim **1**, wherein a third origin of the third three-dimensional rectangular coordinates sys-

tem (x_3, y_3, z_3) in the first three-dimensional rectangular coordinates system (x_1, y_1, z_1) is (0, 0, -100).

5. The system as claimed in claim **4**, wherein an z_3-axis positive direction rotates about 15 degrees along a counterclockwise direction relative to an z_1-axis positive direction.

6. The system as claimed in claim **1**, wherein a fourth origin of the fourth three-dimensional rectangular coordinates system (x_4, y_4, z_4) in the first three-dimensional rectangular coordinates system (x_1, y_1, z_1) is (0, -160.83, 209.49).

7. The system as claimed in claim **6**, wherein an z_4-axis positive direction rotates about 0 degrees along a counterclockwise direction relative to an z_1-axis positive direction.

8. The system as claimed in claim **1**, wherein the sixth-order polynomial freeform

$$Z = \frac{cr^2}{1+\sqrt{1-(1+k)c^2r^2}} + b_1 y + b_2 x^2 + b_3 y^2 + b_4 x^2 y + b_5 y^3 + b_6 x^4 + b_7 x^2 y^2 + b_8 y^4 + b_9 x^6 + b_{10} x^4 y^2 + b_{11} x^2 y^4 + b_{12} y^6$$

$$r^2 = x^2 + y^2,$$

surface of x_2y_2 is: wherein, z represents surface sag, c represents surface curvature, k represents conic constant, and b_1 (i=1, 2, . . . , 11, 12) represents an ith term coefficient; c=4.57e−04, k=0.048, b_1=0.0951, b_2=5.26e−06, b_3=7.90e−05, b_4=3.41e−07, b_5=3.97e−07, b_6=5.54e−10, b_7=1.29e−09, b_8=6.84e−10, b_9=0, b_{10}=0, and b_{12}=0.

9. The system as claimed in claim **1**, wherein the spherical surface of x_4y_4 is:

$(x-A)^2+(y-B)^2+(z-c)^2=r^2$, A=0, B=−160.83, C=209.49, and r=−988.48.

10. The system as claimed in claim **1**, wherein a fifth three-dimensional rectangular coordinates system (x_5, y_5, z_5) is defined by an image sensor location, a fifth origin of the fifth three-dimensional rectangular coordinates system (x_5, y_5, z_5) in the first three-dimensional rectangular coordinates system (x_1, y_1, z_1) is (0, -145.13, -174.41), and an z_5-axis positive direction rotates about 10 degrees along a counterclockwise direction relative to an z_1-axis positive direction.

11. The system as claimed in claim **1**, wherein a length of the off-axis hybrid surface three-mirror optical system along a y_1-axis is about 430 millimeters.

12. The system as claimed in claim **11**, wherein a length of the off-axis hybrid surface three-mirror optical system along a z_1-axis is about 400 millimeters.

13. The system as claimed in claim **1**, wherein a field angle of the hybrid surface three-mirror optical system is about 3°×6°.

14. The system as claimed in claim **13**, wherein an angle in an horizontal direction is in a range from about −1.5° to about 1.5°.

15. The system as claimed in claim **13**, wherein an angle in a vertical direction is in a range from about −16° to about −10°.

16. The system as claimed in claim **1**, wherein an effective focal length of the hybrid surface three-mirror optical system is about 220 millimeters.

17. The system as claimed in claim **1**, wherein an F-number is about 2.2.

18. An off-axis hybrid surface three-mirror optical system comprising:

a primary mirror located on an outgoing light path of rays;

a secondary mirror located on a first reflected light path, which is emitted from the primary mirror;

a tertiary mirror located on a second reflected light path, which is emitted from the secondary mirror; and

an image sensor located on a third reflected light path, which is emitted from the tertiary mirror;

wherein a first three-dimensional rectangular coordinates system (x_1, y_1, z_1) is defined in space; relative to the first three-dimensional rectangular coordinates system (x_1,y_1, z_1), a second three-dimensional rectangular coordinates system (x_2 y_2 z_2) is defined by a primary mirror location, a third three-dimensional rectangular coordinates system (x_3, y_3, z_3) is defined by a secondary mirror location, and a fourth three-dimensional rectangular coordinates system (x_4 y_4, z_4) is defined by a tertiary mirror location; in the second three-dimensional rectangular coordinates system (x_z, y_z, z_2), a reflective surface of the primary mirror is a sixth-order polynomial freeform surface of x_2y_2; in the third three-dimensional rectangular coordinates system (x_3, y_3, z_3), a reflective surface of the secondary mirror is a sixth-order polynomial aspheric surface of x_3y_3; and in the fourth three-dimensional rectangular coordinates system (x_4, y_4, z_4), a reflective surface of the tertiary mirror is a spherical surface of x_4y_4.

19. The system as claimed in claim **18**, wherein the sixth-order polynomial freeform

$$Z = \frac{cr^2}{1+\sqrt{1-(1+k)c^2r^2}} + b_1 y + b_2 x^2 + b_3 y^2 + b_4 x^2 y + b_5 y^3 + b_6 x^4 + b_7 x^2 y^2 + b_8 y^4 + b_9 x^6 + b_{10} x^4 y^2 + b_{11} x^2 y^4 + b_{12} y^6$$

$$r^2 = x^2 + y^2,$$

surface of x_2y_2 is: wherein, z represents surface sag, c represents surface curvature, k represents conic constant, and b_i(i=1, 2, . . . , 11, 12) represents an ith term coefficient; c=4.57e−04, k=0.048, b_1=0.0951, b_2=5.26e−06, b_3=7.90e−05, b_4=3.41e−07, b_5=3.97e−07, b_6=5.54e−10, b_7=1.29e−09, b_8=6.84e−10, b_9=0, b_{10}=0, and b_{12}=0.

* * * * *